FTMP-based Simulation of Twin Nucleation and Substructure Evolution under Hypervelocity Impact

***Tatsuya Okuda[1], Kazuhiro Imiya[2], and Tadashi Hasebe[3]**

[1]Graduate School of Engineering, Kobe University, 1-1 Rokkodai, Nada, Kobe 657-8501, Japan.
[2]Iga Campus, Mori Seiki Co. Ltd, 201 Midai, Iga City, Mie 519-1414, Japan.
[3]Department of Mechanical Engineering, Faculty of Engineering, Kobe University, 1-1 Rokkodai, Nada, Kobe 657-8501, Japan.

*Corresponding author: 137t316t@stu.kobe-u.ac.jp

Abstract

The deformation twinning model based on Field Theory of Multiscale Plasticity (FTMP) utilizes the twin degrees of freedom via an incompatibility tensor, incorporating it into the hardening law of the FTMP-based crystalline plasticity framework, which is then further implemented into a finite element code. The FTMP-based model is adapted to a single slip-oriented FCC single crystal sample, and preliminary simulations are conducted under static conditions to confirm the model's basic capabilities. The simulation results exhibit nucleation and growth of twinned regions, accompanied by serrated stress response with softening. Simulations under hypervelocity impact conditions are also conducted to investigate the model's descriptive capabilities of induced complex substructures composing of both twins and dislocations. The simulated nucleation of twins is examined in detail by using duality diagrams in terms of the flow-evolutionary hypothesis.

Keywords: Deformation twinning, Twin nucleation, Hypervelocity impact, Crystalline plasticity, Multiscale modeling, Field theory

Introduction

Twinning, which is a predominant deformation mechanism in hexagonal close-packed (HCP) metals, is also observed in deformation of body-centered cubic (BCC) metals as well as deformation of face-centered cubic (FCC) metals under impact. In polycrystalline metals, twinning is known to act as an accommodation to redundant deformation attributed to geometrical constraints. Since the earliest evidence of deformation twinning, several efforts have been undertaken to incorporate twinning, mainly for the purpose of predicting textures and stress-strain responses. However, there is no established twinning model with the capability of simulating the nucleation and growth of twinned regions, together with the resulting lattice rotation altogether.

The conventional crystal plasticity-based FEM is capable of simulating slip-induced deformation, though it is incapable of taking into account the formation of dislocation substructures, which form via additional microscopic degrees of freedom. Since dislocation substructures are known to effectively alter the mechanical properties of materials, it is crucial to consider the formation of dislocation substructures via dislocation interaction as well as other phenomenon occurring in the microscopic scale, in order to sufficiently measure plastic deformation.

The Field Theory of Multiscale Plasticity (FTMP) (Hasebe, 2008a,b) is a comprehensive approach that enables direct treatments of the evolutions of "inhomogeneity," instead of merely linking microscopic events to macro-plasticity. Inhomogeneity within a particular field can be expressed completely with "torsion" and "curvature"; in continuum mechanics, torsion (or dislocation density tensor) is given as the first derivative of distortion, and curvature (or incompatibility tensor) is given as the second derivative of strain. These notions are applied to metallic materials as non-

Riemannian plasticity (Kondo, 1955), and form the foundation of the differential geometry-based field theory incorporated in FTMP. The past results imply that locally-stored strain is transformed to incompatibility, which is released in various size scales, and that the resulted evolution of the inhomogeneity field follows; this process is proposed as the Flow-Evolutionary Hypothesis in FTMP. In FTMP-based modeling, the incompatibility tensor model, which corresponds to the degree of freedom (DOF) of deformation modes, is implemented in the hardening law of the crystalline plasticity framework, and this makes it possible for the present model to explicitly analyze multiscale evolution of inhomogeneity as well as interactions between scales.

The FTMP-based deformation twinning model to be proposed here incorporates the twin DOF via the incompatibility tensor, which is implemented in a hardening law independent from that of slip, is capable of simulating concurring slip and twin deformations. The present model qualitatively simulates the formation of a lenticular twin nucleus and its growth, together with the resulting lattice rotation, softening and serrated stress response in analyses conducted in low temperatures under static condition. The results demonstrate that twinning can be associated to the evolution of the inhomogeneity field, though further examination of the basic capabilities of the model and assessment on the evolution of inhomogeneity based on incompatibility is necessary.

Deformation twinning is also observed under impact and hypervelocity impact conditions. When stressed under such extremely high strain rates, FCC metals such as Nickel exclusively form diverse substructures composing of mixed twins and dislocations, which vary according to the applied pressure and pulse durations. Associated with the morphology of the induced substructure, the mechanical properties of materials can be significantly altered.

In this work, the basic capabilities of the FTMP-based deformation twinning model are demonstrated by adaptation to FCC metals, and the simulated nucleation of twins is examined in detail by using duality diagrams in terms of the flow-evolutionary hypothesis (Hasebe, 2013). Simulations under impact conditions are also conducted to investigate the model's descriptive capabilities for reproducing induced complex substructures.

Modeling Deformation Twinning – Kinematics and Constitutive Model

In the present study, the elasto-plastic decomposition by Lee is extended to that including the twin deformation by introducing an intermediate configuration,

$$\boldsymbol{F} = \boldsymbol{F}^{e} \cdot \boldsymbol{F}^{tw} \cdot \boldsymbol{F}^{p} \tag{1}$$

where the deformation gradient tensor for the twinning is represented by $\boldsymbol{F}^{tw}$. Correspondingly, the Jaumann rate of the Kirchhoff stress tensor is given by,

$$\boldsymbol{\tau}_{(J)} = \boldsymbol{C}^{e} : \boldsymbol{d} - \sum_{\alpha=1}^{N} \boldsymbol{R}^{(\alpha)} \dot{\gamma}^{(\alpha)} + \sum_{\bar{\alpha}=1}^{N} \boldsymbol{R}^{tw(\bar{\alpha})} \dot{\gamma}^{tw(\bar{\alpha})} \tag{2}$$

with

$$\begin{cases} \boldsymbol{R}^{(\alpha)} = \boldsymbol{C}^{e} : \boldsymbol{P}^{(\alpha)} + \boldsymbol{\beta}^{(\alpha)} \\ \boldsymbol{\beta}^{(\alpha)} = \boldsymbol{W}^{(\alpha)} \cdot \boldsymbol{\sigma} - \boldsymbol{\sigma} \cdot \boldsymbol{W}^{(\alpha)} \end{cases} \text{and} \begin{cases} \boldsymbol{R}^{tw(\bar{\alpha})} = \boldsymbol{C}^{e} : \boldsymbol{P}^{tw(\bar{\alpha})} + \boldsymbol{\beta}^{tw(\bar{\alpha})} \\ \boldsymbol{\beta}^{tw(\bar{\alpha})} = \boldsymbol{W}^{tw(\bar{\alpha})} \cdot \boldsymbol{\sigma} - \boldsymbol{\sigma} \cdot \boldsymbol{W}^{tw(\bar{\alpha})} \end{cases} \tag{3}$$

The strain rate due to deformation twin is assumed to be driven by the evolution of the incompatibility tensor field for the twinning mode, $\eta_{tw}^{(\bar{\beta})} \equiv \left(\boldsymbol{t}^{tw(\bar{\beta})} \otimes \boldsymbol{s}^{tw(\bar{\beta})} \right) : \boldsymbol{\eta}$, i.e.,

$$\dot{\gamma}^{tw(\bar{\alpha})} = Q_{\bar{\alpha}\bar{\beta}}^{tw} \left| \dot{\gamma}_{prev}^{tw(\bar{\beta})} \right| \tag{4}$$

$$Q_{\overline{\alpha}\overline{\beta}}^{tw} = \delta_{\overline{\alpha}\overline{\beta}} \cdot F\left(\eta_{tw}^{(\overline{\beta})}\right) \cdot \left\langle 1 - \frac{\left|F\left(\eta_{tw}^{(\overline{\beta})}\right)\right|}{F_{sat}^{tw}} \right\rangle \quad (0 \le a \le 1) \tag{5}$$

Thus, the activation of twinning in the present model depends solely on the evolution of $F\left(\eta_{tw}^{(\overline{\beta})}\right)$, which denotes the FTMP-based incompatibility term defined as,

$$F\left(\eta_{tw}^{(\overline{\alpha})}\right) = \operatorname{sgn}\left(\eta_{tw}^{(\overline{\alpha})}\right) \frac{\overline{k}}{p_\eta} \left(\frac{l_{twin}}{b}\left|\eta_{tw}^{(\overline{\alpha})}\right|\right)^{1/2} \tag{6}$$

Flow-Evolutionary Hypothesis in FTMP

The "flow-evolutionary" hypothesis asserts a generalized law for the evolutions of the inhomogeneous fields and the attendant local plastic flow accompanied by the energy dissipation. The notion "duality" between fluctuating hydrostatic stress and deviatoric strain fields introduced in FTMP (Hasebe, 2006) can be embodied by this law, although it still is a "working hypothesis," deserving further verifications and validations. Specifically, it represents an interrelationship between the locally-stored strain energy (fluctuation part) and the local plastic flow (in the form of incompatibility tensor field η_{ij}) as has been discussed in the context of polycrystalline plasticity (Aoyagi and Hasebe, 2007). The hypothesis is given by Eq. (7). The details of "flow-evolutionary" hypothesis is found in the work by Hasebe (2013). A brief derivation process is described below.

$$\eta_{ij} = \kappa \delta T_{ij} \tag{7}$$

Here, η_{ij} and δT_{ij} are the incompatibility tensor, which represents inhomogeneity within a particular field, and the fluctuation of the energy-momentum tensor, which represents locally-stored internal energy, respectively. Let κ be the transport coefficient which represents the energy flow between strain and locally-stored energy. Four-dimensional representation of the incompatibility tensor is given as the derivation of local elastic strain ε^e

$$\eta_{ab} = -\in_{aklp} \in_{bmnp} \partial_k \partial_m \varepsilon_{lm}^e \tag{8}$$

where the indices a, b denote spatio-temporal components, i.e., $a, b = 1, 2, 3, 4$, with 4 being time. In this study, we focus on the duality relation based on the temporal components of η_{ij} and δT_{ij}, i.e., η_{44} and T_{44}, given by Eq. (9).

$$\eta_{44} = \kappa \delta T_{44} = \kappa \delta (K + U^e) \tag{9}$$

In Eq. (9), T_{44} on the right-hand side coincides with the Hamiltonian of the system, i.e., the total energy, consisting of the kinetic energy K and the local strain U^e. For the left-hand side, on the other hand, by utilizing the generalized definition of the cross product for 4D (McDavid and McMullen, 2006), we have,

$$\eta_{44} = \in_{4klp} \in_{4mnp} \partial_k \partial_m \varepsilon_{ln}^p = \eta_{KK} \tag{10}$$

In this study, in order to investigate the energy flow in twinning, we examine the local strain U^e in addition to the fluctuation of the local strain δU^e.

Hardening Law and Field Theoretical Strain Gradient terms

As mentioned above, the present constitutive model incorporates the contributions of $\alpha^{(\alpha)}$ and $\eta^{(\alpha)}$ through the hardening ratio $Q_{\alpha\beta}$ as,

$$Q_{\alpha\beta} = f_{\alpha k} S_{\beta k} + \delta_{\alpha\beta}\left\{1 + F\left(\alpha^{(\alpha)}; \eta^{(\alpha)}\right)\right\} \tag{11}$$

where $f_{\alpha k}$ represents the dislocation interaction matrix, and $S_{\beta k}$ expresses history matrix further given as an increasing function of plastic work done by the effective stress that responsible for dislocation processes, e.g.,

$$S_{\alpha\beta} = \tanh\left[\frac{(W_p)^*_{\alpha\beta}}{(W_p)^*_{sat}}\right] \text{with } (W_p)^*_{\alpha\beta} = \delta_{\alpha\beta}(W_p)^*_{(\beta)} \tag{12}$$

where $(W_p)^*_{(\beta)}$ defines the plastic work done by the effective stress for dislocation processes only (excluding other contributions), e.g.,

$$(W_p)^*_{(\beta)} = \int (\dot{W}_p)^*_{(\beta)} dt \text{ with } (\dot{W}_p)^*_{(\alpha)} = \langle \tau^{(\alpha)} - \tau^{*(\alpha)}_{Peierls} \rangle \cdot \dot{\gamma}^{(\alpha)} \tag{13}$$

Here, $F_k\left(\alpha_k^{(\beta)}; n_k^{(\beta)}\right) \equiv F_k\left(\alpha_k^{(\beta)}\right) + F_k\left(n_k^{(\beta)}\right)$ expresses the field theoretical "strain gradient terms" given respectively as (Aoyagi and Hasebe, 2007),

$$\begin{cases} F\left(\alpha_{slip}^{(\alpha)}\right) = \dfrac{\bar{k}}{p_\alpha}\left(\dfrac{\left|\alpha^{(\alpha)}\right|}{b}\right)^{1/2} \\ F\left(\eta_{slip}^{(\alpha)}\right) = \operatorname{sgn}(\eta^{(\alpha)})\dfrac{\bar{k}}{p_\eta}\left(\dfrac{l_{defect}}{b}\left|\eta^{(\alpha)}\right|\right)^{1/2} \end{cases} \tag{14}$$

where p_α, p_η are coefficients related with the contributions of the $\alpha_k^{(\beta)}$ and $\eta_k^{(\beta)}$, the resolved components of α_{ij} and η_{ij} respectively, to the change in the effective cell size d_{cell}, while l_{defect} represents the characteristic length of the defect field considered, e.g., $l_{defect} = b$ for dislocation dipoles and $l_{defect} = 10^{-6}$ m for dislocation substructures like cells. In Eq. (11), the hardening law can be obtained without the effect of the strain gradient terms, which take into account the slip-induced inhomogeneity which occurs with deformation.

Results and Discussion

Basic Capability of FTMP-based Twinning Model

Here we incorporate a $24 \times 24\mu m^2$ finite element model with 24×24 crossed-triangle elements, assuming single crystal Cu. The nodes at the top end are given a total displacement of 7.2 μm, corresponding to 30% tensile strain of the model, at the strain rate of 1.0×10^{-3} s^{-1} in plane strain condition. The model surface is set to be in parallel to (1 2 1), while the loading axis is oriented in $[1\ 2\ \bar{5}]$.

Firstly, simulations are conducted incorporating precursor inhomogeneity due to slip by implementing the FTMP-η model, i.e., $F(\alpha)$ and $F(\eta)$, into the hardening law of the model. The simulated contour diagrams for frequency of twinning in the primary twinning plane $(\bar{1}\ 1\ 0)$ are shown in the upper part of Fig.1. The results exhibit nucleation and the subsequent evolution of lenticular twinned regions at the center of the sample, accompanied by serrated stress response and softening. The frequency of twinning is given as the total number of simulation time steps in which the twinning plane meets a critical resolved shear stress condition, the point at which the twin model becomes operative. In the present model, the activation of twins at nucleation sites is essentially controlled by the evolution of precursor inhomogeneities driven by slip, and this implies that the twinning behavior of materials is greatly affected by slip and strain history.

To investigate this implication, simulations are repeated under conditions without precursor inhomogeneity, i.e., $F_1(\alpha), F_2(\eta) \to 0$. The simulation results are shown in the bottom part of Fig. 1. In this case, nucleation is delayed until $\varepsilon = 0.163$, and growth is ultimately initiated around $\varepsilon = 0.170$, not from the center, but from the upper/lower edges. There is also a decrease in the overall flow stress, though this is attributed mainly to the absence of $F(\alpha)$, which associates the

slip-induced formation of dislocation substructures and its effect on hardening, and not to the difference in twinning behavior.
Figure 2 compares evolving contours for twinned regions, together with the incompatibility term $F(\eta_{twin})$, between the two cases: with and without precursor inhomogeneity. When there is no precursor inhomogeneity, we can see that weak evolution of slip-induced inhomogeneity, which is displayed as the mild modulation in $F(\eta_{twin})$, tends to inhibit the twin nucleation within the sample. Twinning in this case occurs from non-uniformity associated with boundary conditions.

The results eloquently demonstrate some of the prominent capabilities of the proposed twinning model, where (1) natural representations of twin nucleation (in the sense that it requires no artificial imperfections that promote the activation of twins), (2) the nucleated twins grow while forming a lenticular shape, and (3) the attendant stress-strain response was accompanied by serration and softening. In addition, the nucleation of twinning was obtained exclusively by incorporating precursor inhomogeneity, and thus our theory implies that the formation of twin nuclei within metallic crystals is largely influenced by the strain history.

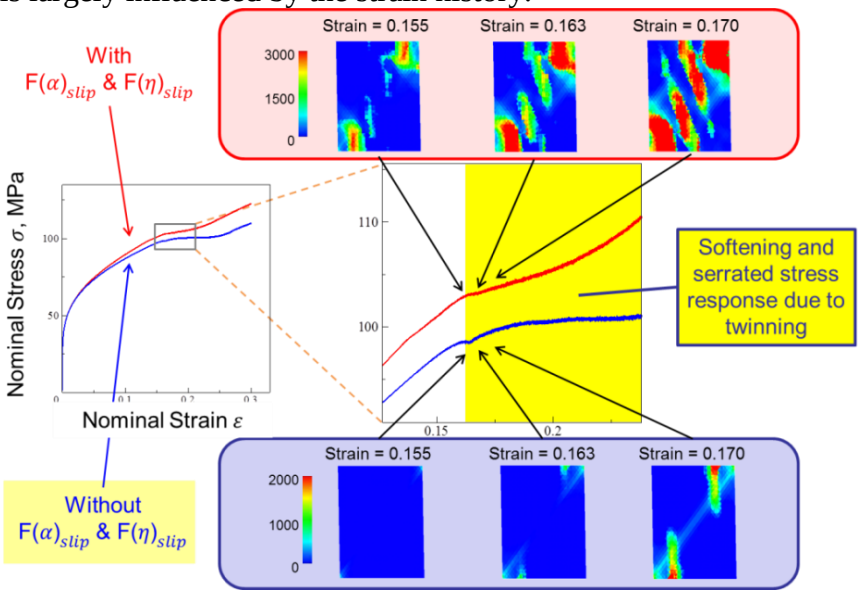

Figure 1. Stress-strain responses comparing effect of precursor inhomogeneity on twin evolution.

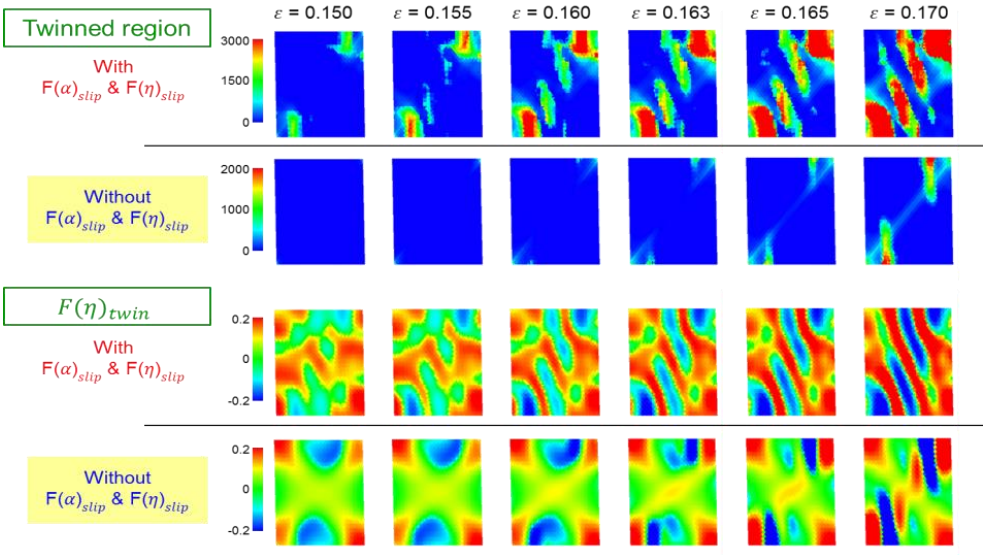

Figure 2. Comparison of twin domains (top) and incompatibility (bottom) for simulations with and without dislocation- and incompatibility-induced hardening.

Examination of Twin Nucleation via Duality Diagram

In this section, we investigate the simulated nucleation and growth of the twinned region in detail via the duality diagram in terms of the flow-evolutionary hypothesis. As explained previously, the duality diagram represents an interrelationship between the local plastic flow (energy dissipation) in the form of incompatibility tensor η_{KK} and the locally-stored elastic strain energy U^e. Since the present model incorporates the twin DOF as an alternative mode for releasing locally-stored strain energy, it is assumed that the differences in the evolution, e.g. nucleation and the subsequent growth of the twinned regions is reflected in the process of converting local strain energy to incompatibility.

In order focus on the twin nucleation phenomena, we limit the area of examination to the center of the model to exclude the influence of intruding twinning from the upper/lower edges. Here we compare the two cases: with and without twin nucleation. Figure 3 illustrates the targeted area together with the simulation results.

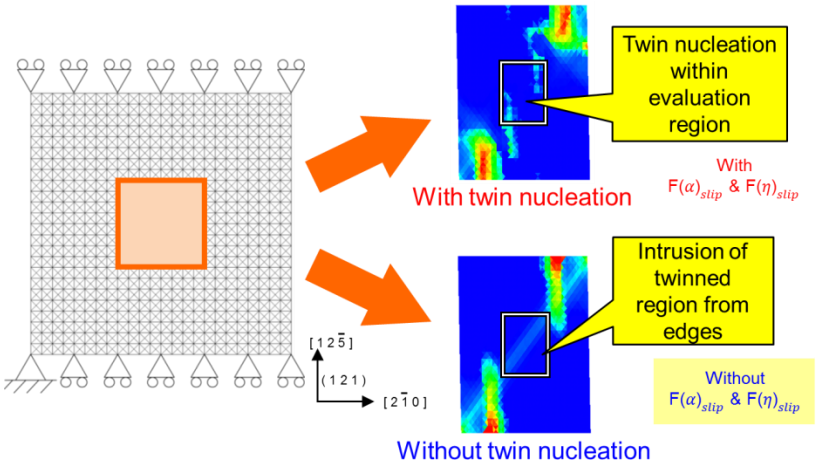

Figure 3. Observation area for duality diagram comparing cases with and without nucleation.

Figure 4 shows the duality diagram, i.e. the duality relation between incompatibility tensor η_{KK} and elastic strain energy U^e. The red line represents the case with twin nucleation, whereas the blue line represents the case without twin nucleation. When we compare the two cases, both cases show a sharp rise in η_{KK} as the strain energy U^e increases, and the case with nucleation shows a much earlier onset of rise in η_{KK} than that without nucleation. To examine this difference more in detail, we enlarge the portion in the duality diagram where the sharp rises occur, where we can clearly confirm marked differences between the two cases. For the case with nucleation, we observe a relatively gradual rise in η_{KK}, followed by a sharp rise occurring at the point of nucleation, indicated with the solid circle. The pre-growth of η_{KK} corresponds to the evolution of the precursor inhomogeneity, as discussed earlier. The case without nucleation, on the other hand, yields a much smaller growth rate of η_{KK}, which is followed by a sharp increase not by twin nucleation, but by the intrusion of twinned regions into the targeted area, the point of which is indicated with the open circle.

From the energetic point of view, the duality diagram provides the following insight; in the case with twin nucleation, a rapid release of energy that has been stored elastically into the twin degrees of freedom results in twin nucleation and subsequent growth. By using the duality diagram, we are able to visualize the twinning evolution (nucleation and growth) in terms of associated energy flow (how elastically-stored strain energy is converted to localized plastic flow in the form of twinning). Our results demonstrate the effectiveness of the duality diagram as a quantitative approach to twinning behavior.

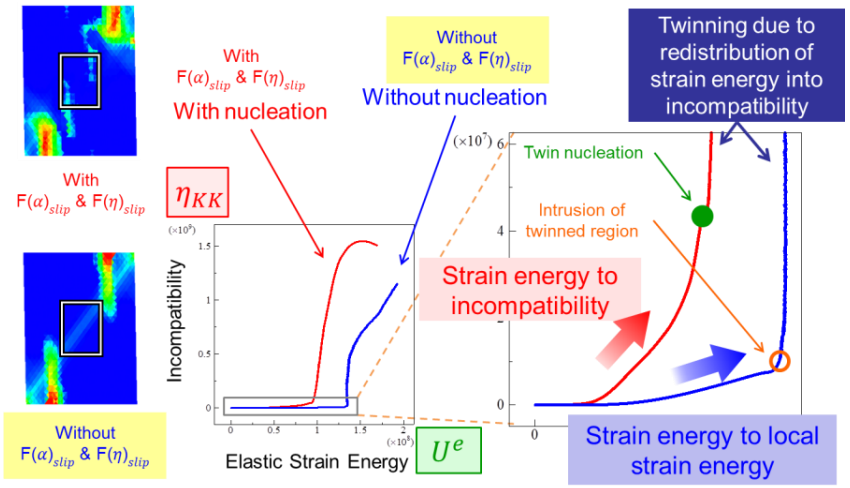

Figure 4. Duality diagram for FCC copper simulation results comparing cases with and without nucleation.

Application of FTMP-based Twin Model to Impact Conditions

Here we conduct simulations that investigate the model's descriptive capabilities under impact conditions. The analyses are carried out as a preliminary step to the model's application to hypervelocity impact conditions, which is to be conducted in future works. When stressed under hypervelocity impact conditions, a wide variety of complex substructures composing both of twins and dislocations, whose morphology varies according to imparted pressure and pulse duration, form within materials. The present model aims to simulate the formation of such substructures, together with their significant effects on the mechanical properties. The simulations in this section are carried out statically, and the dynamic effect is not considered. The analytical model employed in the analysis is the same as that in the previous sections, except that the strain rate is set to $\dot{\varepsilon} = 1.0 \times 10^3$ /s, which corresponds to impact condition.

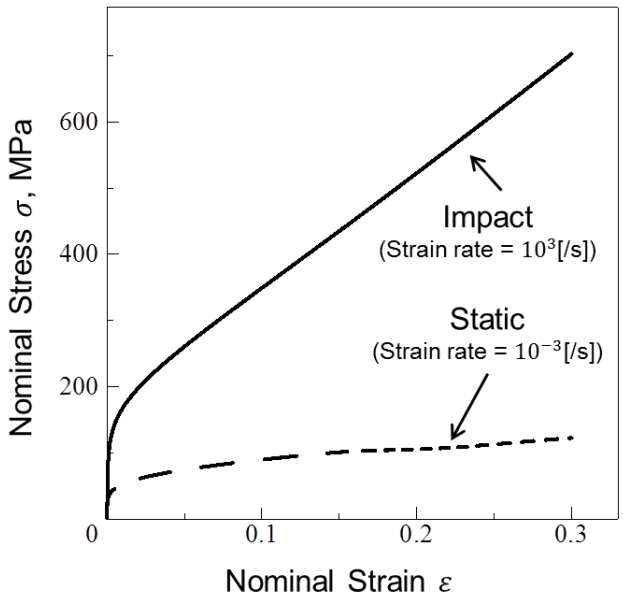

Figure 5. Simulated stress-strain curves comparing results for impact and static conditions.

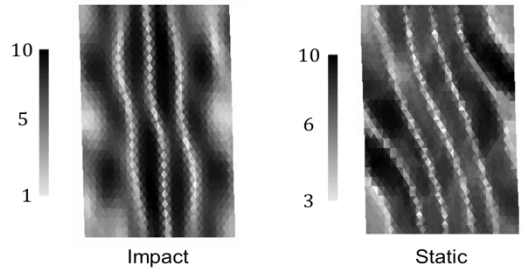

Figure 6. Contour diagrams for dislocation density comparing results under impact and static conditions.

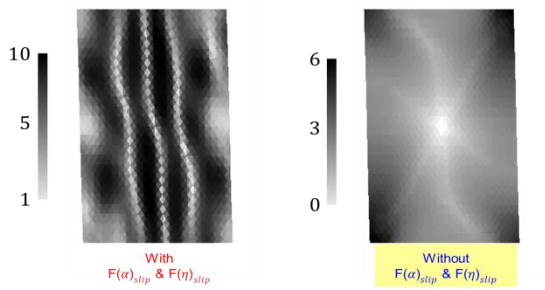

Figure 7. Contour diagrams for dislocation density comparing effect of precursor inhomogeneity.

Firstly, we examine the simulation results by comparing with those obtained in static conditions. Figures 5 and 6 show simulated stress-strain responses and contour diagrams of dislocation density, respectively, for both impact and static conditions. It is apparent that by increasing the strain rate, the flow stress is greatly raised, and the resulting pattern in dislocation density is also altered.

Secondly, the simulations are repeated without precursor inhomogeneity, in order to examine the characteristics of the present model under impact conditions. Figure 7 compares contour diagrams of dislocation density for the two typical cases: with and without precursor inhomogeneity. The result-with precursor inhomogeneity exhibits a banded pattern clearly, notwithstanding the absence of the precursor inhomogeneity results in no notable patterns. The simulation results imply that even under impact loading conditions, the deformation behavior is greatly influenced by the strain history, i.e., slip-induced inhomogeneity.

Conclusions

In this work, we demonstrate the basic capabilities of the FTMP-based deformation twinning model, investigate the twin nucleation process by using duality diagrams, and apply the present model to analyses carried out under impact conditions. The foregoing results demonstrate some prominent capabilities of the proposed twinning model:

- Natural representations of twin nucleation are possible in the sense that no artificial imperfections which promote the onset of twinning are required.
- Nucleation and subsequent growth into lenticular shapes of twinned regions is realistically captured.
- Stress-strain responses accompanied by overall softening and serration are predicted.

Also, by examining the nucleation process in detail based on the duality diagram representation, we can readily visualize the energy flow associated with the nucleation and the subsequent growth of the twinning. With the application of the present model to impact conditions, we obtain dislocation density contour with different morphology from those attained in static conditions, implying that the present model has a potential of simulating twinning-induced complex substructures under a wide variety of loading conditions.

Acknowledgements

A support from Army Research Laboratory (ARL) under Contract No. FA5029-13-P-0043 is greatly acknowledged.

References

Aoyagi, Y. and Hasebe, T. (2007), New Physical Interpretation of Incompatibility and Application to Dislocation Substructure Evolution., *Key Engineering Materials*, 340-341, pp. 217-222.

Hasebe, T. (2013), FTMP-based Flow-Evolutionary Hypothesis and Its Applications., Proc. APCOM2013 (this issue).

Hasebe, T. (2008a), Interaction Fields Based on Incompatibility Tensor in Field Theory of Plasticity-Part I: Theory-. *Interaction and Multiscale Mechanics*, 2-1, pp. 1-14.

Hasebe, T. (2008b), Interaction Fields Based on Incompatibility Tensor in Field Theory of Plasticity-Part II: Application-. *Interaction and Multiscale Mechanics*, 2-1, pp. 15-30.

Hasebe, T. (2006), Multiscale Crystal Plasticity Modeling based on Field Theory., *CMES*, 11-3, pp. 145-155.

Imiya, K. (2011), Modeling of Twin Deformation based on Field Theory of Multiscale Plasticity., Graduation thesis, Kobe University.

Kondo, K. (1955), Non-Riemannian Geometry of Imperfect Crystals from a Macroscopic Viewpoint., *RRAG Memoirs*, 1D-1, pp. 458-469.

McDavid, A.W. and McMullen, C.D. (2006), Generalizing Cross Products and Maxwell's Equations to Universal Extra Dimensions., arXiv:hep-ph/0609260.